13th World Conference on Earthquake Engineering
Vancouver, B.C., Canada
August 1–6, 2004
Paper No. 46

LONG STROKE MAGNETIC DAMPER FOR A SEISMIC ISOLATION DEVICE FOR MACHINES

Kenichiro OMATA[1], Toshiharu ARAKAWA[2] and Yousuke MEZAKI[3]

SUMMARY

A new type of magnetic damper using racks and pinions has been developed. The magnetic damper is composed of two racks, two pinions, a copper disk and rare–earth magnets. The damper has a long stroke and is suitable for a seismic isolation device for a machine, which is installed on a high story in a building. The seismic responses, the optimum damping ratio and the response spectra of a machine–isolation system installed on the 6th story in a 7–story building were calculated. The calculated results showed the effectiveness of the damper and the necessity of a long stroke damper. The trial magnetic damper was made and the resisting force characteristics were measured. The experimental results agreed fairly well with the theoretical results. The seismic responses of a one–degree–of–freedom system consisting of a mass, a coil spring and the trial damper, which corresponds to a machine–isolation system, were measured using an electro–hydraulic type vibration machine. The experimental results agreed with the calculated results to some degree and the validity of the calculations was confirmed.

INTRODUCTION

Magnetic damper has the advantages of the linear damping force characteristics, non-contact mechanism and being resistant to heat, and has been studied by many researchers (for example Schieber [1], Weinberger [2], Nagaya et al. [3–5], Asami, et al. [6]). The magnetic damping is not so strong, so that it is effective in dynamic vibration absorbers which require less damping (for examples Seto, et al. [7], Kobayashi, et al. [8], Aida, et al. [9], Matsuhisa, et al. [10]). The authors proposed two types of magnetic dampers with a force magnifying mechanism: one is a damper using a ball screw (Ohmata, et al. [11]) and the other is a damper using a lever–type displacement–force magnifying mechanism (Matsuoka, et al. [12]).

In this paper, the authors propose a new type of magnetic damper using racks and pinions. The damper is composed of two racks, two pinions, a copper disk and rare–earth magnets. It is possible for the damper to make a long stroke by using long racks. The seismic responses, the optimum damping ratio and the response spectra of a machine–isolation system that consists of a mass, a coil spring and the magnetic

[1] Professor, Meiji University, Kawasaki, Japan. Email: ohmata@isc.meiji.ac.jp
[2] Associate professor, Meiji University, Kawasaki, Japan.
[3] Graduate student, Meiji University, Kawasaki, Japan.

damper and is installed on the 6th story in a 7–story building were calculated. The trial damper was made and the resisting force characteristics were measured and compared with the theoretical results. The trial damper was attached to a one–degree–of–freedom system consisting of a mass, a coil spring, and the frequency responses and the seismic responses of the mass were measured using an electro–hydraulic type vibration machine. The experimental results are compared with the calculated results, and the effects of vibration suppression of the damper and the validity of the calculations are substantiated.

SEISMIC RESPONSE ANALYSES OF A 7–STORY BUILDING AND A MACHINE–ISOLATION SYSTEM IN THE BUILDING

Seismic Responses of a 7–Story Building and the Optimum Damping Ratio of the Isolation System

Let us consider a case in which a machine (a mass) is installed on the 6th story in a 7–story building through a seismic isolation system consisting of a spring and a viscous damper, and the foundation is subject to a seismic excitation $\ddot{z}$ as shown in Fig. 1. Assuming the seismic responses of the building are independent of the motion of the machine, the equations of motion of the building are given by

$$\begin{aligned} & m_i\ddot{x}_i + c_i\left(\dot{x}_i - x_{i-1}\right) + c_{i+1}\left(\dot{x}_i - \dot{x}_{i+1}\right) \\ & \quad + k_i\left(x_i - x_{i-1}\right) + k_{i+1}\left(x_i - x_{i+1}\right) = -m_i\ddot{z} \quad (i = 2 \sim 6) \\ & m_7\ddot{x}_7 + c_7\left(\dot{x}_7 - \dot{x}_6\right) + k_7\left(x_7 - x_6\right) = -m_7\ddot{z} \\ & m_1\ddot{x}_1 + c_1\dot{x}_1 + c_2\left(\dot{x}_1 - \dot{x}_2\right) + k_1x_1 + k_2\left(x_1 - x_2\right) = -m_1\ddot{z} \end{aligned} \tag{1}$$

where x_j (j=1~7) is the displacement of the jth story relative to the foundation, m_j, c_j, k_j are the mass, damping coefficient and stiffness of the jth story respectively. The equation of motion of the machine–isolation system is given by

$$m\ddot{u} + c\dot{u} + ku = -m\ddot{X}_6 \tag{2}$$

where m is the mass of the machine, c and k are the damping coefficient and stiffness of the isolator respectively, u is the relative displacement of the machine, and $\ddot{X}_6\left(= \ddot{x}_6 + \ddot{z}\right)$ is the absolute accelera– tions of the 6th story.

Equations (1), (2) were programmed using the time history analysis in the finite element method "ANSYS/Structural", and the response acceleration waves of the 6th story and the machine–isolation system were calculated. The calculations were carried out changing the value of the damping coefficient c of the viscous damper. The input seismic waves used here are El Centro (1940) NS, JMA Kobe (1995) NS and Akita (1983) NS normalized to be 5.0 m/s^2 at the maximum acceleration. The numerical condition of the building is given in Table 1 and that of the machine–isolation system is m=100 kg, k=1000 N/m and the natural period=2.0 s. The 1st and 2nd natural periods of the building are 0.548 s and 0.208 s, respectively.

The calculated results are shown in Figs. 2 and 3. Figure 2 is the response waves of the 6th story. It will be seen from Fig. 2 that the maximum accelerations of the 6th story are 2.5~2.7 times greater than the maximum input accelerations. Figure 3 shows the relation between the damping ratio $\varsigma\left(= c/2\sqrt{mk}\right)$ and the maximum acceleration of the machine. It is apparent from Fig. 3 that the optimum damping ratio is about ζ=0.16 regardless of input seismic waves. The maximum relative displacement of the system when ζ takes the optimum value was 120~250 mm in the calculations. It means that the damper should have a long stroke of more than 500 mm. Taking the calculated results into consideration, the trial damper was designed to have the damping ratio ζ of 0.16.

Response Spectra of the Machine–Isolation System

Next, the response spectra (the relation between the maximum acceleration and the natural period) of the machine–isolation system were calculated. It was assumed in the calculations that the damper has the

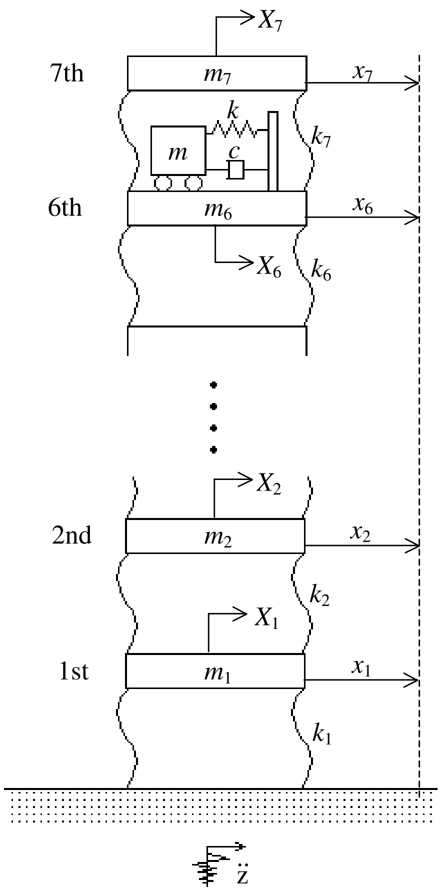

Fig.1 Analytical model

Table 1 Analytical condition

Story	Mass [$\times 10^3$kg]	Stiffness [$\times 10^3$kN/m]
7	568	761
6	400	873
5	424	1323
4	433	1323
3	433	1364
2	441	1593
1	441	1587
Internal damping ratio		0.01

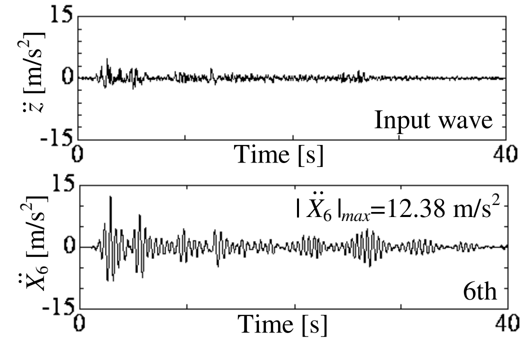

(a) El Centro NS 5.0 m/s^2

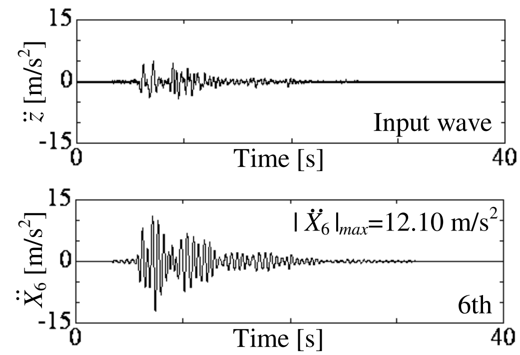

(b) Kobe NS 5.0 m/s^2

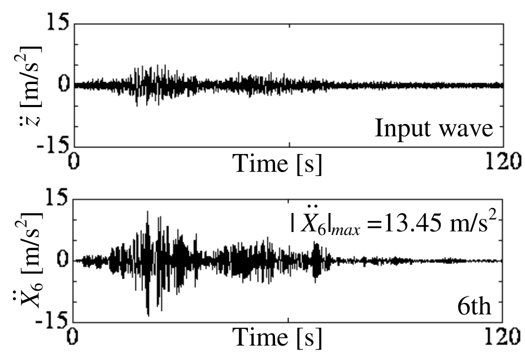

(c) Akita NS 5.0 m/s^2

Fig.2 Input and response acceleration waves

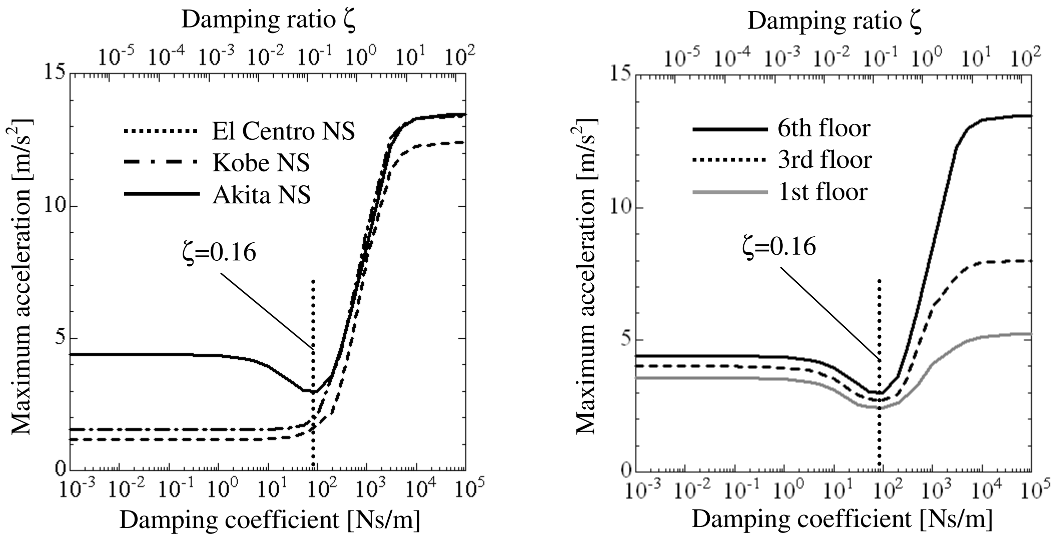

(a) Maximum accelerations of 6th story (El Centro NS, Kobe NS, Akita NS, 5 m/s^2)

(b) Maximum accelerations of three stories (Akita NS, 5 m/s^2)

Fig.3 Relation between damping ratio and maximum acceleration

optimum damping ratio. The results of the calculations for three seismic waves are shown in Fig. 4. It can be seen from Fig. 4 that the damper is particularly effective in suppressing the maximum acceleration of the machine–isolation system whose natural period is in the region of 0.3~1.4 s.

CONSTRUCTION AND RESISTING FORCE OF THE MAGNETIC DAMPER

Figure 5 shows the construction of the magnetic damper using racks and pinions. The magnetic damper consists of two racks, two pinions, a copper disk, rare–earth magnets, linear bearings, guide bars, push rods and rod–ends. The rare–earth magnets are arranged on both sides of the copper disk along a circle of radius R in non–contact with the copper disk. When a relative linear motion is made between two rod–ends, the copper disk rotates because of the racks and pinions. Since the copper disk rotates across the magnetic fluxes due to the rare–earth magnets, the eddy–current damping force proportional to the relative velocity is generated in the copper disk.

If a conductive plate moves across a magnetic flux at velocity v, the damping force f_m is given by (Nagaya, et al. [3], Asami, et al. [6])

$$f_m = (B^2 A h c_0 / \rho) v \tag{3}$$

where B is the magnetic flux density, A the area of a magnetic flux, h the thickness of the conductive plate, ρ the resistivity of the conductive plate and c_0 the dimensionless parameter decided by the shape of both the magnetic flux and the conductive plate. The total force F of the magnetic damper is given by

$$F=(nB^2 A h c_0 / \rho)\lambda^2 v + f_c \,\mathrm{SIGN}(v) \tag{4}$$

where n is the number of the magnetic fluxes, f_c the friction force between racks and pinions, $\lambda=R/r$ the magnifying ratio (radius ratio of the circle of the magnetic fluxes to the pinion) and SIGN(v) is the sign function which takes –1 or 1 corresponding to a minus or plus sign of v.

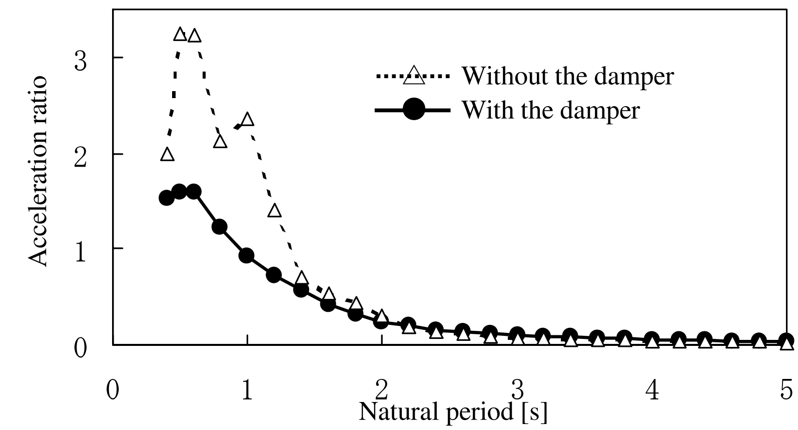

(a) El Centro NS

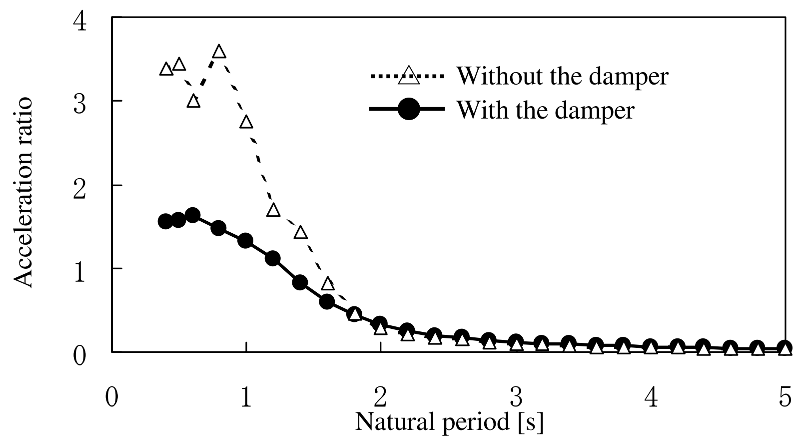

(b) JMA Kobe NS

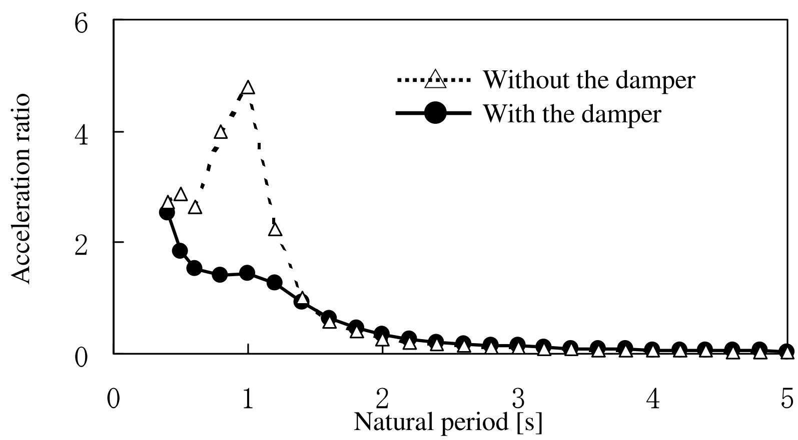

(c) Akita NS

Fig.4 Response spectra of a machine-isolation system

RESISTING FORCE CHARACTERISTICS OF THE TRIAL DAMPER

The trial magnetic damper was made using the 500 mm racks and the Nd–Fe–B magnets with a diameter of 12 mm and a thickness of 10 mm. The experimental condition of the damper is given in Table 2. The trial damper was attached between a mechanical vibration machine and a rigid wall through a load cell, and the force–displacement curves of the damper when it was subject to sinusoidal displacements of amplitudes 1, 30 mm and frequencies 0.5, 1.0, 1.5 Hz were measured.

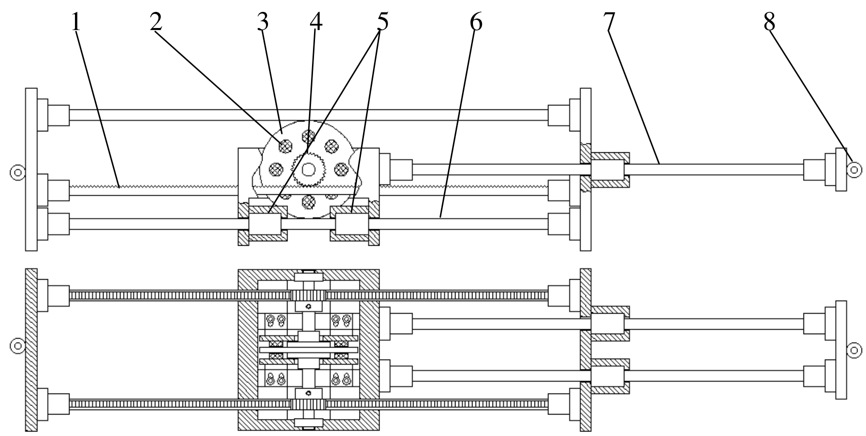

1 Rack 2 Rare-earth magnet 3 Copper plate 4 Pinion
5 Liner motion bearing 6 Guide bar 7 Push rod 8 Rod end

Fig.5 Construction of the magnetic damper

Table 2 Experimental condition of the magnetic damper

Damper	Length of rack	500 mm
	Width	150 mm
	Height	150 mm
	Mass	7.5 kg
	Stroke	± 150 mm
	Radius of pinion	15 mm
Magnet	Material	Nd-Fe-B
	Size	$\phi 12\times 10$ mm
	Open flux B	0.5 T
Copper disk	Radius	45 mm
	Thickness h	5 mm
	Resistivity ρ	1.69×10^{-8} Ωm
	Coefficient C_0	0.44

The experiments were carried out with two different numbers of magnets, i.e. 4 pairs (8 magnets) and 8 pairs (16 magnets). The experimental results are shown in Fig. 6. It will be seen from Fig. 6 that the damper gives about the same resisting force characteristics as Eq. (4) even in small amplitude. The friction force f_c is 0.7 N with 4 pairs of magnets and 1.1 N with 8 pairs of magnets, and f_c may be disregarded as compared to magnetic damping force in case of vibrations with large amplitude.

FREQUENCY RESPONSES OF A ONE–DEGREE–OF–FREEDOM SYSTEM SUPPORTED WITH THE DAMPER

The trial damper was attached to a one–degree–of–freedom system consisting of a mass and a coil spring as shown in Fig. 7, which is equivalent to a machine–isolation system, and the frequency responses of the mass were measured using an electro–hydraulic type vibration machine. The experimental condition of the vibration system is given in Table 3, and the experimental results together with the calculated results are shown in Fig. 8. The equation of motion in this case has the same form as Eq. (2) except that a sinusoidal excitation $\ddot{z}$ $(= -a\omega^2 \cos\omega t)$ is used instead of $\ddot{X}_6$. It is apparent from Fig. 8 that the damper is effective in suppressing the resonance and the isolation system has the effect of vibration suppression at frequencies above 0.75 Hz. The calculated results agree fairly well with the experimental results and the validity of the calculations was confirmed.

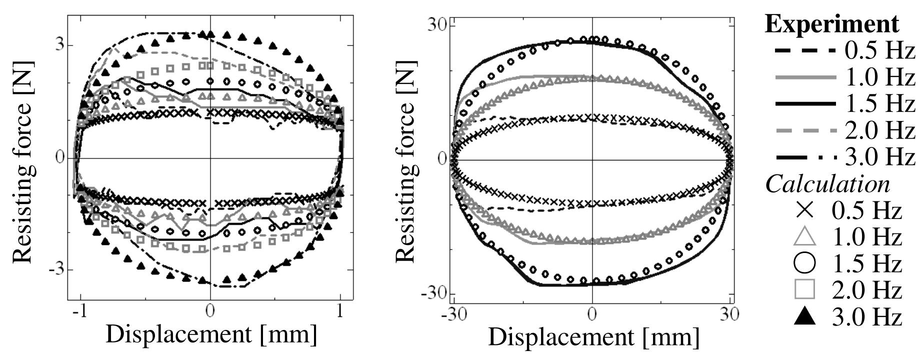

Amplitude 1 mm **Amplitude 30 mm**

(a) 4 pairs of magnets (8 magnets)

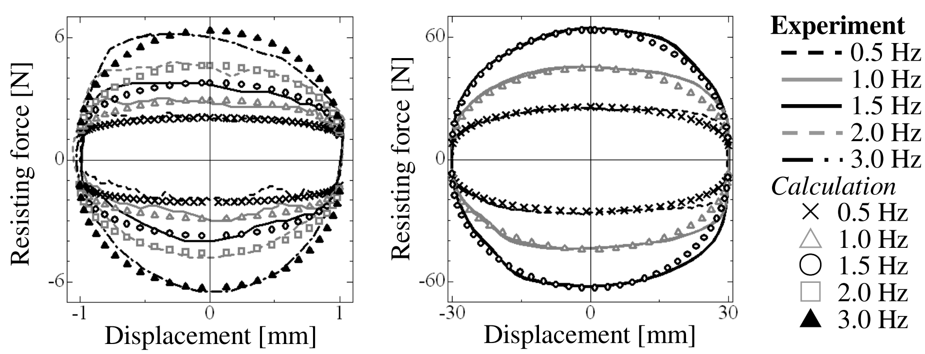

Amplitude 1 mm **Amplitude 30 mm**

(b) 8 pairs of magnets (16 magnets)

Fig.6 Resisting force characteristics of the magnetic damper

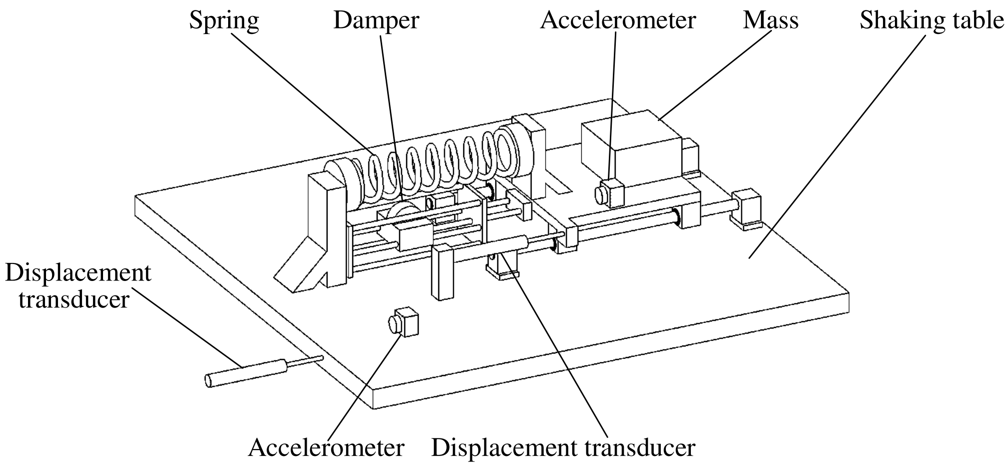

Fig.7 Experimental apparatus of the 1 DOF model

Table 3 Experimental condition of the 1 DOF model

Mass	86.5 kg
Stiffness	932 N/m
Friction	4.4 N
Natural period	1.89 s

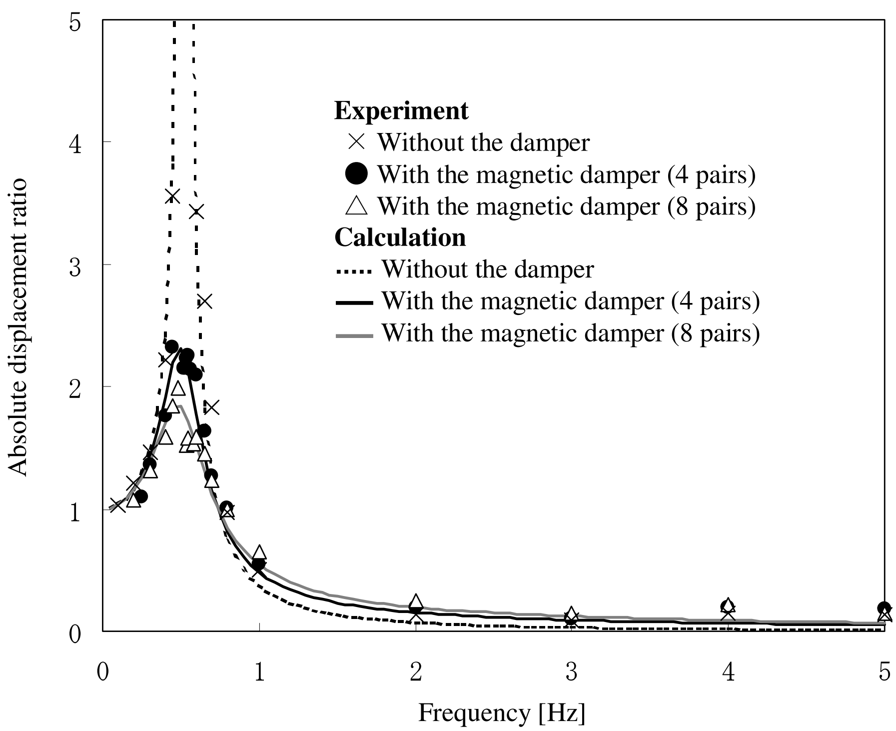

Fig.8 Frequency responses

SEISMIC RESPONSES OF A ONE–DEGREE–OF–FREEDOM SYSTEM SUPPORTED WITH THE DAMPER

Next, the El Centro (1940) NS component normalized to be 1.0, 1.5, 2.0, 2.5, 3.0, 3.5, 4.0 m/s^2 at the maximum acceleration were inputted to the electro–hydraulic type vibration machine, and the response acceleration and relative displacement of the mass of the one–degree–of–freedom system were measured by a servo–type accelerometer and an inductance–type displacement transducer respectively. The experiments were carried out with the damper having 4 pairs and 8 pairs of magnets and without the damper. The maximums of the responses are given in Table 4 and Fig. 9 and the examples of the response waves are shown in Fig. 10 together with the calculated results. It will be seen from Table 4, Fig. 9 and Fig. 10 that the damper has slight various effects in suppressing the vibration of the machine. The reason is that the natural period of the one–degree–of–freedom system is about 2.0 s as pointed out Section 2.2. It is also apparent from Table 4 and Fig. 10 that the experimental results agree with the calculated results to some degree and the propriety of the calculations was substantiated.

CONCLUSIONS

In this paper, a new type of magnetic damper using racks, pinions and rare–earth magnets was proposed. The resisting force characteristics of the damper, the frequency and seismic responses of a machine–isolation system with the magnetic damper and the effects of vibration suppression of the damper were discussed experimentally and numerically. The results may be summarized as follows:

Table 4 Maximums of the responses (El Centro NS)

	Maxima of the responses: upper $\lvert\ddot{X}\rvert_{max.}$ [m/s^2], lower $\lvert u\rvert_{max.}$ [mm]					
Maximum input accel.	Without the damper		With the magnetic damper (4 pairs)		With the magnetic damper (8 pairs)	
$\lvert\ddot{z}\rvert_{max}$ [m/s^2]	Exp.	Cal.	Exp.	Cal.	Exp.	Cal.
1.0	0.38	0.27	0.29	0.20	0.40	0.28
	21.47	24.70	14.14	14.81	9.35	12.85
1.5	0.51	0.40	0.35	0.30	0.45	0.43
	33.65	37.05	20.20	22.22	16.87	19.27
2.0	0.60	0.53	0.45	0.40	0.60	0.57
	50.26	49.40	29.13	29.63	23.94	25.69
2.5	0.76	0.67	0.54	0.50	0.70	0.71
	62.69	61.75	35.95	37.04	30.58	32.11
3.0	0.93	0.80	0.64	0.60	0.85	0.85
	78.45	74.10	46.17	44.44	37.73	38.54
3.5	1.06	0.93	0.70	0.70	0.95	1.00
	91.31	86.46	53.58	51.85	44.97	44.96
4.0	1.18	1.06	0.80	0.80	1.03	1.12
	105.28	98.81	61.67	59.26	51.53	51.38

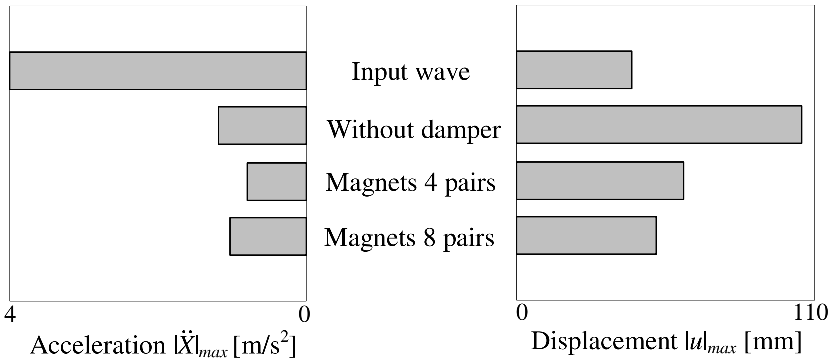

Fig.9 Maximums of the responses (El Centro NS 4.0 m/s^2)

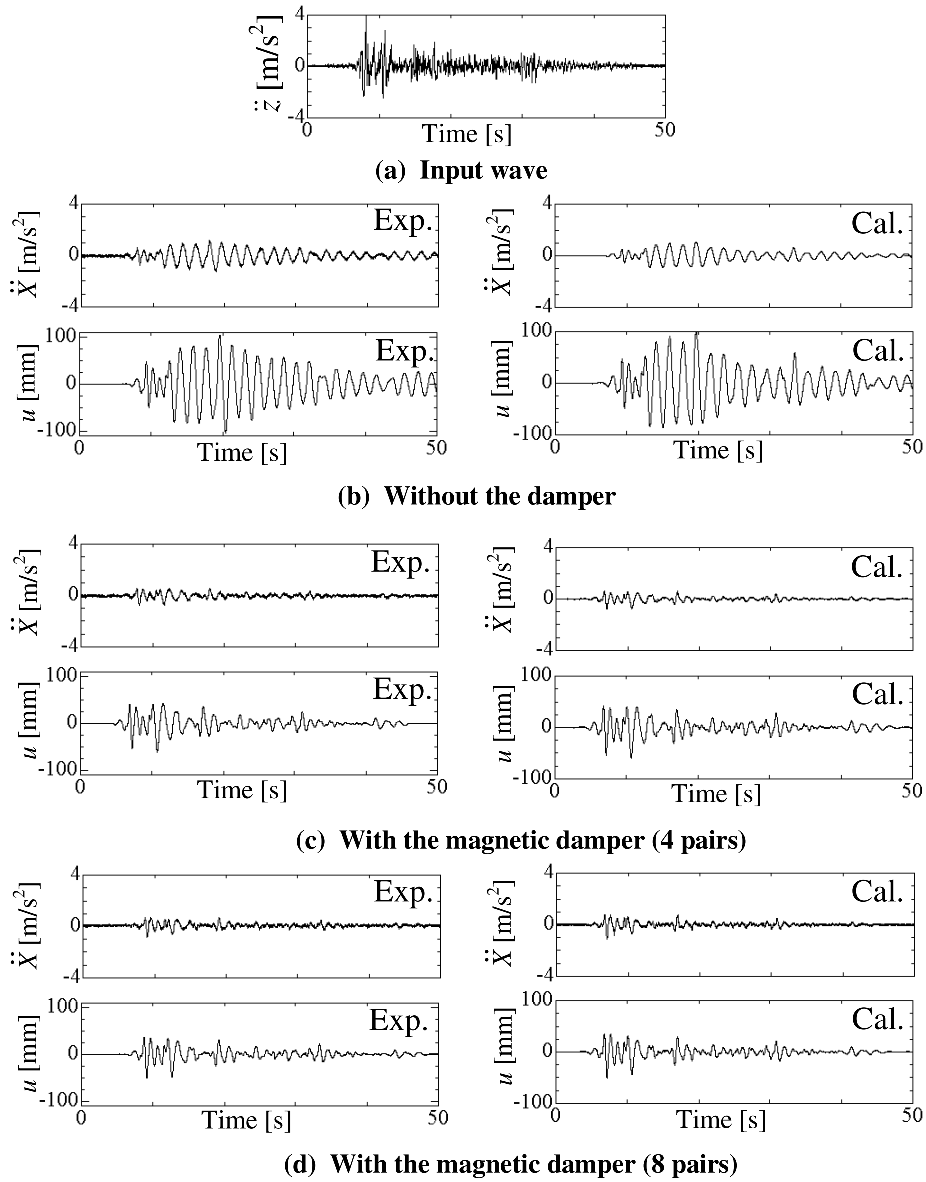

Fig.10 Time histories of $\ddot{X}$ and u (El Cenrto NS 4.0 m/s^2)

(1) The resisting force of the trial magnetic damper is given by the sum of the magnetic damping force and the friction force. However, the friction force is negligible as compared to the magnetic damping force in case of a vibration with large amplitude
(2) The magnetic damping force is increased λ^2 times ($\lambda=R/r$; the radius ratio of the circle of the magnetic fluxes to the pinion).
(3) The magnetic damper is able to make a long stroke of more than 500 mm and gives about the same resisting force characteristics even in small amplitude.
(4) The magnetic damper is particularly effective in suppressing the maximum acceleration of the machine–isolation system whose natural period is in the region of 0.3~1.4 s.
(5) The optimum damping ratio of the damper applied to a machine–isolation system installed on the 6th story in a 7–story building is about $\zeta=0.16$ regardless of input seismic waves.
(6) The experimental results of the frequency responses and seismic responses of a one–degree–of–freedom system with the magnetic damper showed the effectiveness of the magnetic damper.
(7) The experimental results agree with the calculated results to some degree and the propriety of the calculations was confirmed.

This research was supported by the Grant-in-Aid for Scientific Research (C) of the Ministry of Education, Science and Culture of Japan and the Institute of Science and Technology, Meiji University. These supports are gratefully appreciated.

REFERENCES

1. Schieber D. "Optimal Dimensions of Rectangular Electromagnet for Braking Purpose." IEEE Trans. on magnetics 1975; MAG–11(3): 948–952.
2. Weinberger MR. "Drag Force of an Eddy Current Damper." IEEE Trans. on aerospace and electronic systems 1977; AES–13(2): 197–200.
3. Nagaya K, Kojima H. "Shape Characteristics of the Magnetic Damper Consisting of a Rectangular Magnetic Flux and a Rectangular Conductor." Bull. JSME 1982; 25: 1306–1311.
4. Nagaya K, Kojima H. "On a Magnetic Damper Consisting of a Circular Magnetic Flux and a Conductor of Arbitrary Shape. Part I: Derivation of the Damping Coefficients." Trans. ASME 1984; 106: 46–51.
5. Nagaya K, Kojima H. "On a Magnetic Damper Consisting of a Circular Magnetic Flux and a Conductor of Arbitrary Shape. Part II: Application and Numerical Results." Trans. ASME 1984; 106: 52–55.
6. Asami T, Hosokawa Y. "A Practical Expression for Design of a Magnetic Damper (Improvement of Convergence in the Nagaya–Kojima Expression)." Trans. JSME (in Japanese) 1995; 61–582 C: 587–590.
7. Seto K, Yamanouchi M. "On the Effect of a Variable Stiffness–Type Dynamic Absorber with Eddy–Current Damping." Bull. JSME 1978; 21(160): 1482–1489.
8. Kobayashi H, Aida S. "Development of a Houde Damper Using Magnetic Damper." Proc. Vibration Isolation, Acoustics and Damping in Mechanical Systems 1993; ASME DE–Vol.62: 25–29.
9. Aida Y, et al. "Dynamic Vibration Absorber Using Magnetic Spring and Damper." Seismic Engineering 1995; ASME PVP–Vol.312: 439–445.
10. Matsuhisa H, Nishihara O. "Dynamic Vibration Absorber for a Ropeway Carrier." Proc. 1997 ASME Design Engineering Technical Conference; DECT 97/VIB–3944: 85–94.
11. Ohmata K, Yamakawa I. "Ball Screw Type Damper Using Rare–Earth Magnets." Proc. 10th International Workshop on Rare–Earth Magnets and Their Applications 1989; Vol. II: 65–73.
12. Matsuoka T, Ohmata K. "A Study of a Magnetic Damper Using Rare–Earth Magnets and a Pinned Displacement Magnifying Mechanism." International Journal of Applied Electromagnetics and Mechanics 2001/2002; 13: 263–270.